Oxygen Permeation Through a CO_2-Tolerant Mixed Conducting Oxide $(Pr_{0.9}La_{0.1})_2(Ni_{0.74}Cu_{0.21}Ga_{0.05})O_{4+\delta}$

Jun Tang, Yanying Wei, Lingyi Zhou, Zhong Li, and Haihui Wang
School of Chemistry and Chemical Engineering, South China University of Technology, Guangzhou 510640, China

DOI 10.1002/aic.12742
Published online September 1, 2011 in Wiley Online Library (wileyonlinelibrary.com).

A novel K_2NiF_4-type oxide based on $(Pr_{0.9}La_{0.1})_2(Ni_{0.74}Cu_{0.21}Ga_{0.05})O_{4+\delta}$ (PLNCG) dense mixed conducting ceramic membrane was successfully prepared through a sol–gel route. The oxygen permeation flux through the membrane swept by pure CO_2 was comparative to that swept by He. The oxygen permeation and the stability of PLNCG under pure CO_2 were investigated in detail. A membrane with a thickness of 0.8 mm was steadily operated for 230 h with a constant oxygen permeation flux of 0.32 mL/(min cm^2) at 975°C using pure CO_2 as sweep gas. X-ray diffraction shows that PLNCG can maintain its fluorite phase, and no carbonates were observed, even when it was exposed to pure CO_2 for a long time. *AIChE J,* 58: 2473–2478, 2012
Keywords: membrane, mixed conductor, oxygen permeation, separation, CO_2

Introduction

Recently, CO_2 capture and storage technologies have received great interest, because they can reduce the emission of CO_2 which is considered as the main contribution to the global warming.[1–5] So far, postcombustion capture, precombustion separation, and oxyfuel combustion techniques are three major concepts for CO_2 sequestration.[3,4] Mixed oxygen ionic–electronic conducting ceramic (MIEC) membranes have gained increasing attention due to their potential applications in oxygen supply to power stations with CO_2 sequestration (e.g., according to the oxyfuel concept[5–7]) and could be promising for the thermal decomposition of carbon dioxide in combination with the partial oxidation of methane to syngas.[8–12] Many perovskite oxides have been investigated as membranes for oxygen separation. However, there is a main problem for the proper application of perovskite membranes especially. For numerous applications such as the oxyfuel process and hydrocarbon partial oxidations, in which some CO_2 is formed as by-product of an undesired deeper oxidation, the oxygen transporting membranes must sustain their phase stability and oxygen transport property under CO_2-containing atmosphere. Usually, the perovskite-type membranes contain alkaline-earth metals on A site, which tend to react readily with acidic or even amphoteric gases such as SO_2, CO_2, and H_2O to form sulfates,[13,14] carbonates,[15–19] and hydroxides and bicarbonates.[20,21] Arnold et al.[18] observed an immediate stop of the oxygen permeation for $Ba_{0.5}Sr_{0.5}Co_{0.8}Fe_{0.2}O_{3-\delta}$ (BSCF) membrane, when pure CO_2 was used as sweep gas at 875°C. Yang et al.[19] found that the perovskite structure of $La_{0.1}Sr_{0.9}Co_{0.5}Fe_{0.5}O_{3-\delta}$ (LSCF) decomposed to carbonate and metallic oxide phases after CO_2 treatment at 800°C.

Many intensive efforts have been made to develop the CO_2-tolerant ceramic oxygen separation membranes. One effective way is to avoid alkaline-earth metals during the oxides preparation process. Dong et al.[22] reported that $La_{0.85}Ce_{0.1}Ga_{0.3}Fe_{0.65}Al_{0.05}O_{3-\delta}$ (LCGFA) mixed conducting oxide powder maintained full perovskite structure after annealing in 20 vol % CO_2 + He for 100 h at 900°C. Another way is proper doping which can improve the chemical stability of MIECs' structure. Zuo et al.[23] found that Zr-doped $BaCe_{0.8}Y_{0.2}O_{3-\delta}$ shows an improved stability in the CO_2-containing atmosphere. Zeng et al.[24] demonstrated that Ti-doped $SrCo_{0.8}Fe_{0.2}O_{3-\delta}$ (SCF) can effectively increase the tolerance toward the acidic CO_2. Very recently, Luo et al.[25] developed a novel alkaline and cobalt-free dual-phase CO_2-tolerated oxygen permeable membrane, which exhibits good stability under CO_2-containing atmosphere. However, most of those above-mentioned materials have not been tested under pure CO_2 atmosphere, and the oxygen permeation fluxes through the membranes significantly decreased once CO_2-containing gas instead of pure He was introduced into the sweep side.

Recently, Yashima et al.[26] found that a K_2NiF_4-type MIEC material based on $(Pr_{0.9}La_{0.1})_2(Ni_{0.74}Cu_{0.21}Ga_{0.05})O_{4+\delta}$ (PLNCG) exhibits a significant electronic conductivity. They demonstrated that the oxygen permeability of PLNCG using He as sweep gas is quite high in comparison with the conventional $ABO_{3-\delta}$ perovskite-type MIECs in the literature. However, the chemical stability and oxygen permeability under CO_2 were not studied yet. As known, the PLNCG is the alkaline-earth metal-free MIEC materials, and it should exhibit a good stability in an atmosphere containing CO_2. Therefore, in this paper, the chemical stability and oxygen permeability of the PLNCG membrane under pure CO_2 are investigated in detail.

Correspondence concerning this article should be addressed to H. Wang at hhwang@scut.edu.cn.

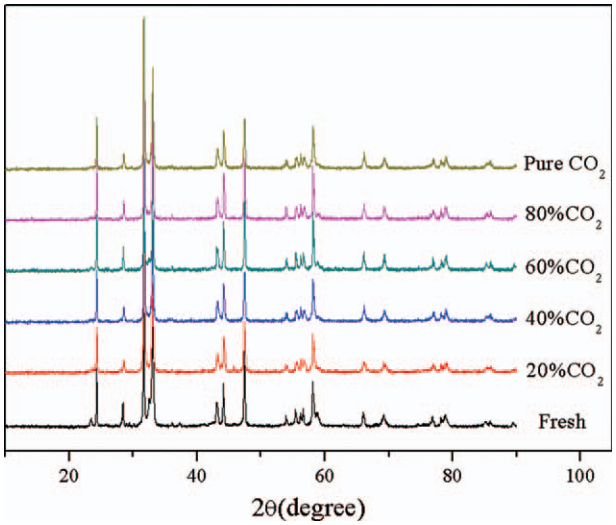

Figure 1. XRD patterns of the PLNCG powder samples before and after exposure to CO_2 with different concentrations at 950°C for 1 h.

[Color figure can be viewed in the online issue, which is available at wileyonlinelibrary.com.]

Experimental

The sol–gel route based on citric acid and EDTA as complexing and gelation agents has been adapted to prepare the powder.[27] Briefly, Ga was dissolved in nitric acid first, and proper amounts of $Pr(NO_3)_3{\cdot}6H_2O$, $La(NO_3)_3{\cdot}6H_2O$, $Ni(CH_3COO)_2{\cdot}4H_2O$, and $Cu(NO_3)_2{\cdot}3H_2O$ were dissolved in water followed by the addition of citric acid, ethylene diamine tetraacetic acid (EDTA), and $NH_3{\cdot}H_2O$. The mixture was then evaporated at 150°C under constant stirring to obtain a dark-green gel. Afterward, the gel was ignited to flame to get the precursor. The precursor was ground and calcined at temperatures up to 950°C with a heating rate of 2°C/min for 10 h. The as-prepared powders were then pressed under 20 MPa to get "green" membranes which were sintered at 1300°C with a dwelling time of 10 h. The densities of the sintered membranes were determined by the Archimedes method using ethanol. Only those membranes that have relative densities higher than 95% are used for oxygen permeation studies.

The phase structure of the as-prepared powder was characterized by X-ray diffraction (XRD, Bruker-D8 ADVANCE, Cu Kα radiation). Thermogravimetric (TG) measurements were performed on a Netzsch 449C simultaneous thermal analyzer under pure CO_2 and N_2.

The oxygen permeation experiments were carried out in a home-made high-temperature permeation cell which was described in detail elsewhere.[28] Membranes were sealed onto a ceramic tube with a ceramic sealant (Huitian Adhesive Enterprise, Hubei, China). After sealing, gases were delivered to the permeation cell by mass flow controllers (model D07-7A/ZM, Beijing Jianzhong Machine Factory, China). Synthetic air was fed to the air side of the membrane, and He/CO_2 was fed to the sweep side. The O_2 concentration of the effluent was continuously detected by an on-line gas chromatograph (GC, Agilent Technologies, 7890A). The GC was frequently calibrated using standard gases like oxygen, helium, and CO_2 to ensure the reliability of the experimental data. Details about the calculation of oxygen permeation flux were presented in our previous paper.[29] In order to analyze the structure of membrane after permeation, XRD characterization was conducted on both surfaces exposed to CO_2 and air.

Results and Discussion

In order to investigate the structural stability of $(Pr_{0.9}La_{0.1})_2(Ni_{0.74}Cu_{0.21}Ga_{0.05})O_{4+\delta}$ under CO_2-containing atmospheres, the phase structures of PLNCG powders treated under different CO_2 concentration atmospheres and temperatures are investigated. Figure 1 shows the XRD patterns of the PLNCG powders before and after exposure to CO_2 with different concentrations at 950°C for 1 h. As shown in Figure 1, the PLNCG powder samples maintain the K_2NiF_4 structure with the increase of the CO_2 concentration even under the pure CO_2. Figure 2 shows the XRD patterns of the PLNCG powder samples after exposure to pure CO_2 at different temperatures for 1 h. The PLNCG powder samples still maintain the K_2NiF_4 structure under pure CO_2 in the temperature range studied, and no carbonate is observed.

Figure 3 shows thermogravimetric curves of BSCF and PLNCG under CO_2/N_2 atmospheres. The samples were heated with ramp rates of 15°C/min and held at the peak temperature of 800°C for 1 h in pure CO_2/N_2 atmosphere with a flow rate of 50 mL/min. It can be seen that the weight change of PLNCG powder under pure CO_2 atmosphere is nearly the same to that under N_2 atmosphere. The mass of PLNCG decreases slightly with the increase of temperature, and no change is observed while dwelling at the maximum temperature. No sharp weight increase or loss of the PLNCG sample indicates that no carbonates generated or decomposed during the temperature increasing. The slight loss of the powder weight under both N_2 and CO_2 atmospheres may be attributed to desorption of interstitial oxygen. For comparison, the TG of BSCF was performed at the same conditions. As we can see that the mass change of BSCF treated in CO_2 is very different from that of PLNCG. About 1.8% mass loss of BSCF is observed when the temperature is below 450°C. Then, the mass of BSCF sample starts to increase at about 450°C and continues to increase till 800°C.

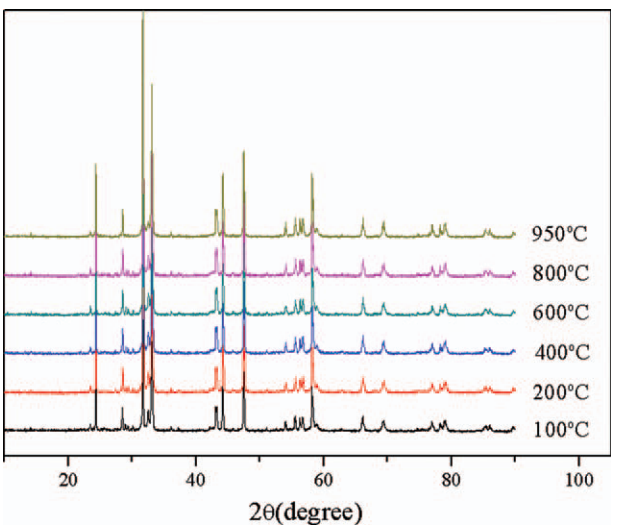

Figure 2. XRD patterns of the PLNCG powder samples after exposure to pure CO_2 at different temperatures for 1 h.

[Color figure can be viewed in the online issue, which is available at wileyonlinelibrary.com.]

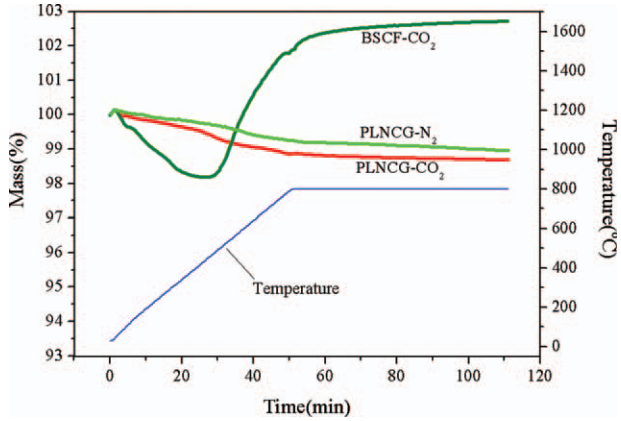

Figure 3. Thermogravimetric curves of BSCF and PLNCG under pure CO_2/N_2 atmosphere.

[Color figure can be viewed in the online issue, which is available at wileyonlinelibrary.com.]

Around 4.5% mass increase is observed during the temperature increases from 450 to 800°C, which is attributed to the formation of carbonate such as $BaCO_3$, as shown in Figure 4. Figure 4 presents the XRD pattern of PLNCG and BSCF after TG measurements. As we can see that both the PLNCG powder treated in CO_2 and N_2 still maintain the K_2NiF_4-type structure. However, the perovskite structure of BSCF is destroyed, and the peaks of $BaCO_3$ and CoO structure appear, as shown in the XRD pattern of the BSCF sample treated in CO_2. Obviously, the BSCF sample is not stable under CO_2 atmosphere due to the formation of $BaCO_3$. Recently, Lin's group reported the O_2 desorption behaviors of SCF and LSCF in CO_2-containing atmosphere.[19,30] The XRD patterns of SCF and LSCF after oxygen desorption show that most of SCF and LSCF decomposed into $SrCO_3$, Fe_2O_3, and CoO, which indicates SCF and LSCF are not stable in CO_2-containing atmosphere. From these comparisons, it is obvious that PLNCG exhibits better stability in the CO_2-containing atmosphere than these perovskite materials containing alkaline-earth metals like BSCF, LSCF, and SCF.

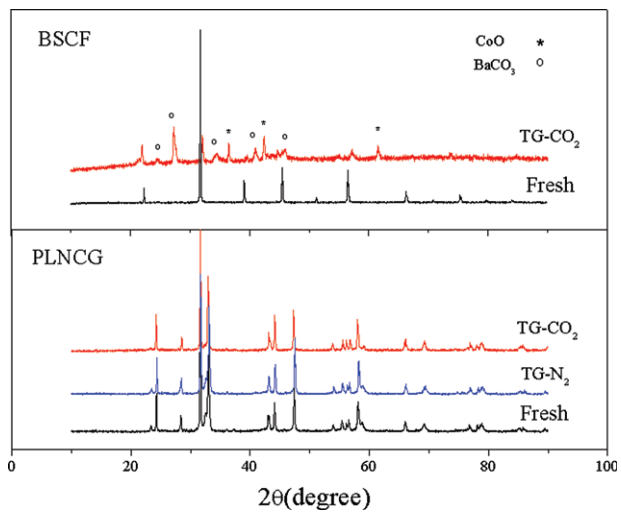

Figure 4. XRD patterns of PLNCG and BSCF powder samples after TG under pure CO_2/N_2 atmosphere.

[Color figure can be viewed in the online issue, which is available at wileyonlinelibrary.com.]

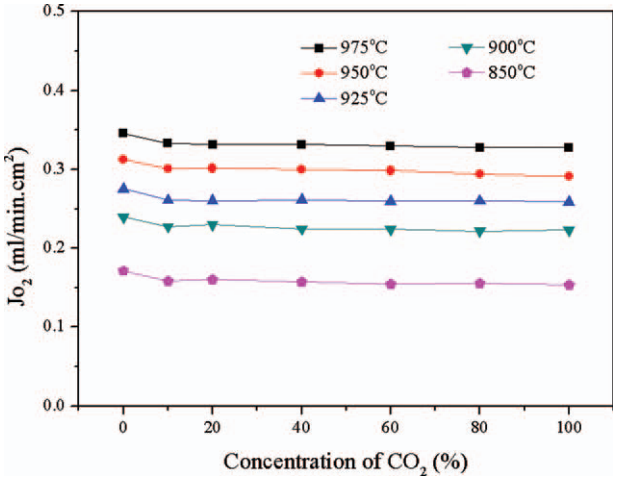

Figure 5. Dependence of oxygen permeation fluxes on the concentration of CO_2 in the sweep gas at different temperatures. F_{air} = 150 mL/min, $F_{He} + F_{CO_2}$ = 30 mL/min.

[Color figure can be viewed in the online issue, which is available at wileyonlinelibrary.com.]

Figure 5 shows the dependence of oxygen permeation flux on the concentration of CO_2 on the sweep side at different temperatures. The total flow rate of sweep gases was kept at 30 mL/min. When CO_2 is introduced into the sweep gas, the oxygen permeation fluxes only slightly decrease. Afterward, with the increase of the content of CO_2, the oxygen permeation fluxes are almost constant. Many previous studies indicate that the oxygen surface-exchange reaction on MIECs is affected by the gas atmospheres. Ten Elshof et al.[31] observed that the activation energy found on $La_{0.7}Sr_{0.3}FeO_{3-\delta}$ in air/CO, CO_2 gradients is much lower than in air/He gradients. Yashiro et al.[32] found that the oxygen surface-exchange reaction on gadolinia-doped ceria is related with the gas species. Therefore, the slight fall of the oxygen flux may attribute to the inhibiting effect of CO_2 on the oxygen surface-exchange reaction; in other words, the presence of CO_2 restricted O_2 desorption from the surface of PLNCG membrane.

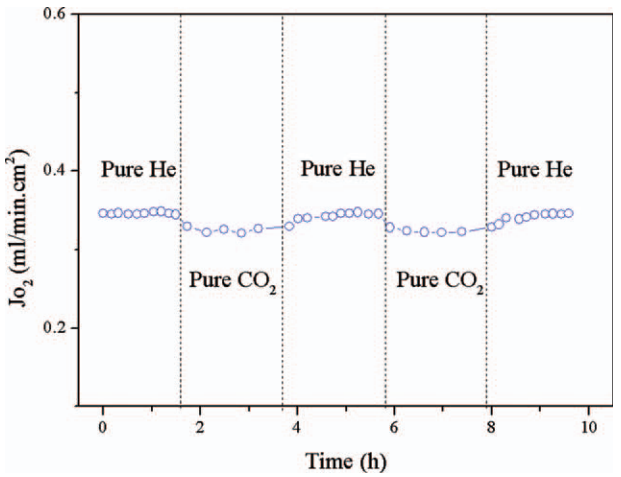

Figure 6. Oxygen permeation fluxes as a function of time while periodically changing the sweep gases. F_{air} = 150 mL/min, $F_{He} + F_{CO_2}$ = 30 mL/min.

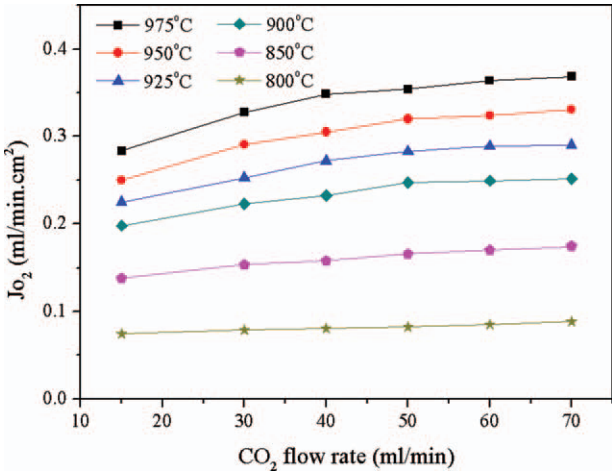

Figure 7. Dependence of oxygen permeation fluxes on the CO_2 flow rates at different temperatures. F_{air} = 150 mL/min.

[Color figure can be viewed in the online issue, which is available at wileyonlinelibrary.com.]

Figure 6 shows the reversibility of oxygen permeation flux through the PLNCG membrane while periodically changing the sweep gas between He and CO_2 at 975°C. If helium is used as the sweep gas, the oxygen permeation fluxes of 0.34 mL/(min cm^2) are obtained. When the sweep gas was changed from He to CO_2, the oxygen permeation flux is 0.32 mL/(min cm^2). Only a slight decrease of the oxygen permeation flux was observed, which is quite different from the alkane-containing perovskite membranes like BSCF. Arnold et al.[18] found an immediate stop of the oxygen permeation for BSCF membrane when pure CO_2 was used as sweep gas at 875°C. Furthermore, when the sweep gas is shifted back to pure helium, the oxygen permeation flux can be recovered.

Some other CO_2-tolerant oxygen permeable membrane materials have been studied in the literature.[22,25] Dong et al.[22] found that the oxygen permeation flux through the

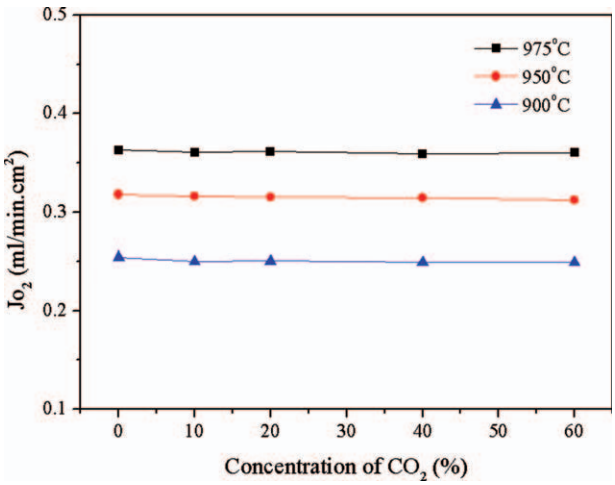

Figure 8. Dependence of oxygen permeation fluxes on the concentration of CO_2 in the feed side at different temperatures. $F_{N_2} + F_{CO_2}$ = 118.5 mL/min, F_{O_2} = 31.5 mL/min, F_{He} = 30 mL/min.

[Color figure can be viewed in the online issue, which is available at wileyonlinelibrary.com.]

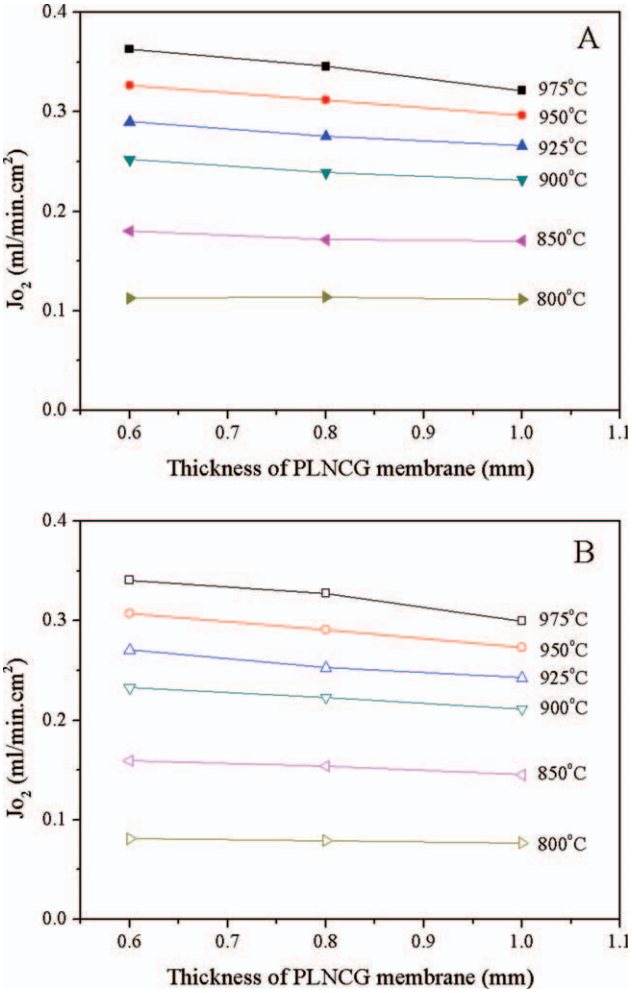

Figure 9. Oxygen permeation fluxes through PLNCG membranes as a function of membrane thickness at different temperatures. A: sweep gas is helium; B: sweep gas is CO_2. F_{air} = 150 mL/min, $F_{He} + F_{CO_2}$ = 30 mL/min.

[Color figure can be viewed in the online issue, which is available at wileyonlinelibrary.com.]

LCGFA membrane with the membrane thickness of 1.0 mm is 0.17 mL/(min cm^2) under air/(He + 20% CO_2) at 950°C. Luo et al.[25] achieved the oxygen permeation flux of 0.27 mL/(min cm^2) through a dual-phase membrane containing 40 wt % $NiFe_2O_4$ and 60 wt % $Ce_{0.9}Gd_{0.1}O_{2-\delta}$ (40NFO–60CGO) at 1000°C, when pure CO_2 is used as sweep gas. It is clear that the PLNCG membrane shows higher oxygen permeation fluxes than those through the LCGFA and 40NFO–60CGO under similar operation conditions.

Figure 7 shows the dependence of the oxygen permeation flux on the swept CO_2 flow rate at different temperatures. It shows that the oxygen permeation flux increased with the increase of the CO_2 flow rate. When the CO_2 flow rate increased from 15 to 70 mL/min, the oxygen permeation fluxes increased from 0.07 to 0.09 mL/(min cm), 0.20 to 0.25 mL/(min cm^2), and 0.28 to 0.37 mL/(min cm^2) at 800, 900, and 975°C, respectively. The oxygen permeation fluxes through the membrane increase with the increase of the CO_2 flow rate, because the higher CO_2 flow rate would dilute the permeated oxygen concentration and lower the oxygen partial pressure on the sweep side.

It was found that the CO_2 in the feed air has a negative influence on the oxygen permeation flux as well as that in the sweep side. For example, Yi et al.[15] found that the oxygen flux through SCF membrane decreased about 3% by 5% CO_2 introducing into the air at 810°C. Tong et al.[16] reported that introduction of CO_2 into air side of $Ba(Co_{0.4}Fe_{0.6-x}Zr_x)O_{3-\delta}$ membrane resulted in an distinct effect on the oxygen permeation flux. When the percentage of CO_2 mixed in air increased, the oxygen permeation flux through $Ba(Co_{0.4}Fe_{0.6-x}Zr_x)O_{3-\delta}$ membrane continued to decrease. Therefore, it is necessary to investigate the influence of CO_2 in the feed air on the oxygen permeation flux through PLNCG membrane. Figure 8 shows the dependence of oxygen permeation flux on the concentration of CO_2 in the feed air at different temperatures. The total flow rate of feed gases was kept at 150 mL/min, and the oxygen partial pressure was kept at 0.21 atm. It can be seen that at different temperatures, the introduction of CO_2 into the feed air has negligible effects on the oxygen permeation fluxes. Even when the concentration of CO_2 in the feed air is 60%, the oxygen permeation fluxes through PLNCG membrane are almost unchanged. This finding demonstrates that PLNCG membrane shows a better tolerance in high concentration of CO_2 atmosphere than the MIEC membranes containing alkaline-earth metals.

Figure 9 shows the oxygen permeation fluxes through the PLNCG membranes with different thicknesses as a function of temperatures using both He and CO_2 as sweep gases. It can be seen that the oxygen permeation fluxes increase distinctly with increasing temperature when both He and CO_2 are used as the sweep gases. Figures 9A, B show that in low-temperature region (800 – 850°C), the oxygen permeation fluxes change little with decreasing membrane thickness. This indicates a significant role of the exchange kinetics to the oxygen permeation process, similar to other K_2NiF_4-type ceramics.[33,34] But, when the operational temperature is over 850°C, the oxygen permeation fluxes increase slightly with decreasing membrane thickness, and the change becomes more obvious with rising temperature, which implies that when temperature increases to 900°C and above, the bulk diffusion plays more and more an important role for the oxygen permeation process through the PLNCG membrane. At

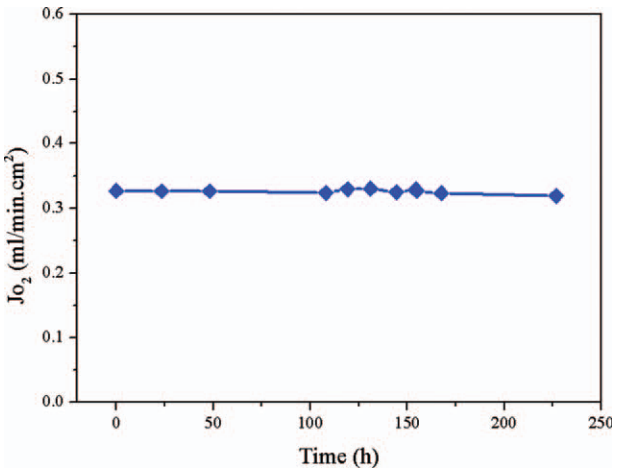

Figure 10. Oxygen permeation flux through PLNCG as a function of time at 975°C. F_{air} = 150 mL/min, F_{CO_2} = 30 mL/min.

[Color figure can be viewed in the online issue, which is available at wileyonlinelibrary.com.]

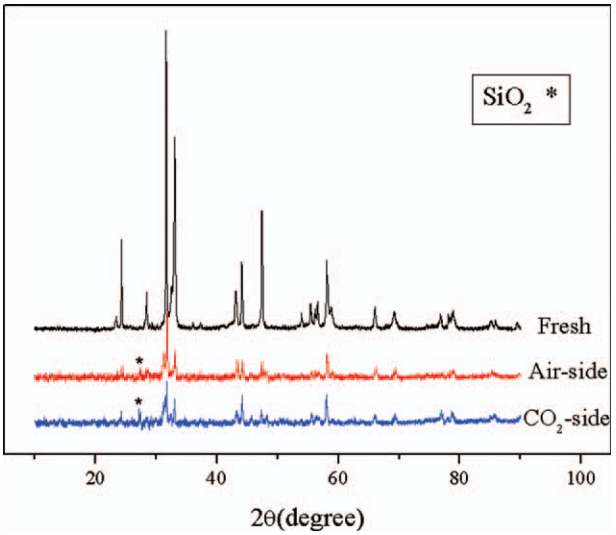

Figure 11. XRD patterns of the fresh and spent PLNCG membranes.

[Color figure can be viewed in the online issue, which is available at wileyonlinelibrary.com.]

975°C, the oxygen permeation fluxes of PLNCG membrane with the thicknesses of 0.6 and 1.0 mm swept by He are 0.36 mL/(min cm^2) and 0.32 mL/(min cm^2), respectively. This small difference shows that surface oxygen exchange is still a main factor for the limiting step of the PLNCG membrane. The oxygen permeation flux can be improved by preparing a porous layer on the membrane surface to improve the surface exchange.[35,36]

Figure 10 shows the oxygen permeation flux through the PLNCG membrane as a function of time at 975°C using pure CO_2 as the sweep gas. It was found that a steady oxygen permeation flux of 0.32 mL/(min cm^2) was obtained, and no decrease of the oxygen permeation flux was found during 230-h oxygen permeation test under pure CO_2. It is not like $Ba_{0.5}Sr_{0.5}Co_{0.8}Fe_{0.2}O_{3-\delta}$ (BSCF) or $La_{0.1}Sr_{0.9}Co_{0.5}Fe_{0.5}O_{3-\delta}$ perovskite materials, where carbonate was formed once CO_2 gas was introduced, and oxygen flux decreased rapidly.[18,19] After the 230-h operation, both sides of the membrane were characterized by XRD. Figure 11 shows the XRD patterns of the membrane surfaces exposed to air and CO_2. It is found that both surfaces of the membrane were kept the K_2NiF_4 structure. The impurity of SiO_2 was observed which came from the ceramic sealant. The membrane surface exposed to the air did not decompose, and no carbonate was observed on the CO_2-side surface. These results demonstrate that the PLNCG membrane exhibits good stability under CO_2 atmosphere and has potential application in oxyfuel techniques.

Conclusions

In this study, PLNCG powder is synthesized by a sol–gel route. It is found that the PLNCG powder can keep its K_2NiF_4 structure after exposed to pure CO_2 at high temperature. For the oxygen permeation experiments, when pure CO_2 is introduced into the sweep side, the oxygen permeation flux through the membrane only slightly decreases. A steady oxygen permeation flux of 0.32 mL/(min cm^2) is obtained during 230-h oxygen permeation at 975°C using pure CO_2 as the sweep gas. After 230-h oxygen permeation, it is found that both sides of the membrane surface keep the

K_2NiF_4 structure. All these results demonstrate that PLNCG is a promising stable material under CO_2 containing atmosphere and has a great potential application in oxyfuel techniques for CO_2 capture and storage technologies.

Acknowledgments

The authors greatly acknowledge the financial support by Natural Science Foundation of China (nos. U0834004 and 20936001), the National Basic Research Program of China (no. 2009CB623406), the Science-Technology Plan of Guangzhou City (2009J1-C511-1), and the Fundamental Research Funds for the Central Universities, SCUT (2009220038).

Literature Cited

1. Metz B, Davidson O, De Coninck H, Loos M, Meyer L. *IPCC Special Report on Carbon Dioxide Capture and Storage*. Cambridge, UK, New York, NY: Working Group III of the Intergovernmental Panel on Climate Change, Cambridge University Press, 2005.
2. Adams D, Davison J. Capturing CO_2, Report, IEA Greenhouse Gas R&D Programme 2007, 2007.
3. Figueroa JD, Fout T, Plasynski S, McIlvried H, Srivastava RD. Advances in CO_2 capture technology—The U.S. Department of Energy's Carbon Sequestration Program. *Int J Greenh Gas Con*. 2008;2:9–20.
4. Gough C. State of the art in carbon dioxide capture and storage in the UK: an experts' review. *Int J Greenh Gas Con*. 2008;2:155–168.
5. Kneer R, Toporov D, Förster M, Christ D, Broeckmann C, Pfaff E, Zwick M, Engels S, Modigell M. OXYCOAL-AC: towards an integrated coal-fired power plant process with ion transport membrane-based oxygen supply. *Energy Environ. Sci*. 2010;3:198–207.
6. Bredesen R, Jordal K, Bolland O. High-temperature membranes in power generation with CO_2 capture. *Chem Eng Process*. 2004;43:1129–1158.
7. Tan XY, Li K, Thursfield A, Metcalfe IS. Oxyfuel combustion using a catalytic ceramic membrane reactor. *Catal Today*. 2008;131:292–304.
8. Tan XY, Li K. Design of mixed conducting ceramic membranes/reactors for the partial oxidation of methane to syngas. *AIChE J*. 2009;55:2675–2685.
9. Gu XH, Jin WQ, Chen CL, Xu NP, Shi J, Ma YH. YSZ–$SrCo_{0.4}Fe_{0.6}O_{3-\delta}$ membranes for the partial oxidation of methane to syngas. *AIChE J*. 2002;48:2051–2060.
10. Fan YQ, Ren JY, Onstot W, Pasale J, Tsotsis TT, Egolfopoulos FN. Reactor and technical feasibility aspects of a CO_2 decomposition-based power generation cycle, utilizing a high-temperature membrane reactor. *Ind Eng Chem Res*. 2003;42:2618–2626.
11. Jiang HQ, Wang HH, Werth S, Schiestel T, Caro J. Simultaneous production of hydrogen and synthesis gas by combining water splitting with partial oxidation of methane in a hollow fiber membrane reactor. *Angew Chem Int Ed*. 2008;47:9341–9344.
12. Yang WS, Wang HH, Zhu XF, Lin LW. Development and application of oxygen permeable membrane in selective oxidation of light alkanes. *Top Catal*. 2005;35(1/2):155–167.
13. Liu SM, Gavalas GR. Oxygen selective ceramic hollow fiber membranes. *J Membr Sci*. 2005;246:103–108.
14. Liu S, Tan X, Shao Z, Diniz da Costa JC. $Ba_{0.5}Sr_{0.5}Co_{0.8}Fe_{0.2}O_{3-\delta}$ ceramic hollow fiber membrane for oxygen permeation. *AIChE J*. 2006;52:3452–3461.
15. Yi JX, Feng SJ, Zuo YB, Liu W, Chen CS. Oxygen permeability and stability of $Sr_{0.95}Co_{0.8}Fe_{0.2}O_{3-\delta}$ in a CO_2 and H_2O containing atmosphere. *Chem Mater*. 2005;17:5856–5861.
16. Tong JH, Yang WS, Zhu BC, Cai R. Investigation of ideal zirconium-doped perovskite-type ceramic membrane materials for oxygen separation. *J Membr Sci*. 2002;203:175–189.
17. Yang Z, Harvey AS and Gauckler LJ. Influence of CO_2 on $Ba_{0.2}Sr_{0.8}Co_{0.8}Fe_{0.2}O_{3-\delta}$ at elevated temperatures. *Scr Mater*. 2009;61:1083–1086.
18. Arnold M, Wang HH, Feldhoff A. Influence of CO_2 on the oxygen permeation performance and the microstructure of perovskite-type $(Ba_{0.5}Sr_{0.5})(Co_{0.8}Fe_{0.2})O_{3-\delta}$ membranes. *J Membr Sci*. 2007;293:44–52.
19. Yang Q, Lin YS, Bülow M. High temperature sorption separation of air for producing oxygen-enriched CO_2 stream. *AIChE J*. 2006;52:574–581.
20. Tanner CW, Virkar AV. Instability of $BaCeO_3$ in H_2O-containing atmospheres. *J Electrochem Soc*. 1996;143:1386–1389.
21. Taniguchi N, Nishimura C, Kato J. Endurance against moisture for protonic conductors of perovskite-type ceramics and preparation of practical conductors. *Solid State Ionics*. 2001;145:349–355.
22. Dong XL, Zhang GR, Liu ZK, Zhong ZX, Jin WQ, Xu NP. CO_2-tolerant mixed conducting oxide for catalytic membrane reactor. *J Membr Sci*. 2009;340:141–147.
23. Zuo CD, Dorris SE, Balachandran U, Liu ML. Effect of Zr-doping on the chemical stability and hydrogen permeation of the Ni–$BaCe_{0.8}Y_{0.2}O_{3-\delta}$ mixed protonic electronic conductor. *Chem Mater*. 2006;18:4647–4650.
24. Zeng Q, Zuo YB, Fan CG, Chen CS. CO_2-tolerant oxygen separation membranes targeting CO_2 capture application. *J Membr Sci*. 2009;335:140–144.
25. Luo HX, Efimov K, Jiang HQ, Feldhoff A, Wang HH, Caro J. CO_2-stable and cobalt-free dual-phase membrane for oxygen separation. *Angew Chem Int Ed*. 2011;50:759–763.
26. Yashima M, Sirikanda N, Ishihara T. Crystal structure, diffusion path, and oxygen permeability of a Pr_2NiO_4-based mixed conductor $(Pr_{0.9}La_{0.1})_2(Ni_{0.74}Cu_{0.21}Ga_{0.05})O_{4+\delta}$. *J Am Chem Soc*. 2010;132:2385–2392.
27. Wang HH, Tablet C, Feldhoff A, Caro J. A cobalt-free oxygen-permeable membrane based on the perovskite-type oxide $Ba_{0.5}Sr_{0.5}Zn_{0.2}Fe_{0.8}O_{3-\delta}$. *Adv Mater*. 2005;17:1785–1788.
28. Wang HH, Tablet C, Feldhoff A, Caro J. Investigation of phase structure, sintering, and permeability of perovskite-type $Ba_{0.5}Sr_{0.5}Co_{0.8}Fe_{0.2}O_{3-\delta}$ membranes. *J Membr Sci*. 2005;262:20–26.
29. Wang HH, Cong Y, Yang WS. Oxygen permeation study in a tubular $Ba_{0.5}Sr_{0.5}Co_{0.8}Fe_{0.2}O_{3-\delta}$ oxygen permeable membrane. *J Membr Sci*. 2002;210:259–271.
30. Rui ZB, Ding JJ, Li YD, Lin YS. $SrCo_{0.8}Fe_{0.2}O_{3-\delta}$ sorbent for high-temperature production of oxygen-enriched carbon dioxide stream. *Fuel*. 2010;89:1429–1434.
31. Ten Elshof JE, Bouwmeester HJM, Verweij H. Oxygen transport though $La_{1-x}Sr_xFeO_{3-\delta}$ membrane II. Permeation in air/CO, CO_2 gradients. *Solid State Ionics*. 1996;89:81–92.
32. Yashiro K, Onuma S, Kaimai A, Nigara Y, Kawada T, Mizusaki J, Kawamura K, Horita T, Yokokawa H. Mass transport properties of $Ce_{0.9}Gd_{0.1}O_{2-\delta}$ at the surface and in the bulk. *Solid State Ionics*. 2002;152–153:469–476.
33. Yaremchenko AA, Kharton VV, Patrakeev MV, Fradea JR. p-Type electronic conductivity, oxygen permeability and stability of $La_2Ni_{0.9}Co_{0.1}O_{4+\delta}$. *J Mater Chem*. 2003;13:1136–1144.
34. Kharton VV, Tsipis EV, Yaremchenko AA, Frade JR. Surface-limited oxygen transport and electrode properties of $La_2Ni_{0.8}Cu_{0.2}O_{4+\delta}$. *Solid State Ionics*. 2004;166:327–337.
35. Wang ZG, Liu H, Tan XY, Jin YG, Liu SM. Improvement of the oxygen permeation through perovskite hollow fibre membranes by surface acid-modification. *J Membr Sci*. 2009;345:65–73.
36. Tan XY, Wang ZG, Liu H, Liu SM. Enhancement of oxygen permeation through $La_{0.6}Sr_{0.4}Co_{0.2}Fe_{0.8}O_{3-\delta}$ hollow fibre membranes by surface modifications. *J Membr Sci*. 2008;324:128–135.

Manuscript received May 13, 2011, and revision received July 5, 2011.